Scientific Research Publishing

Advances in Nanoparticles, 2024, 13, 29-44
https://www.scirp.org/journal/anp
ISSN Online: 2169-0529
ISSN Print: 2169-0510

Numerical Investigation of Heat and Mass Transfer in Nanofluid-Filled Porous Medium

Dalel Helel[1,2], Noureddine Boukadida[2,3]

[1]ISSATS, University of Sousse, Souuse, Tunisia
[2]Laboratory of Metrology and Energy Systems, ENIM, University of Monastir, Monastir, Tunisia
[3]ESSTHS, University of Sousse, Sousse, Tunisia
Email: heleldalel@yahoo.fr

How to cite this paper: Helel, D. and Boukadida, N. (2024) Numerical Investigation of Heat and Mass Transfer in Nanofluid-Filled Porous Medium. *Advances in Nanoparticles*, **13**, 29-44.
https://doi.org/10.4236/anp.2024.133003

Received: May 1, 2024
Accepted: June 25, 2024
Published: June 28, 2024

Abstract

In this work, we numerically study the laminar mixed convection of fluid flow in a vertical channel filled with porous media during the drying process. The porous medium, modeled as a vertical wall, consists of solid and nanofluid phase (Water-Al_2O_3 or Water-Cu), as well as a gas phase. The established model is developed based on Whitaker's theory and resolved by our numerical code using Fortran. Results principally show the influence of various physical parameters, such as nanoparticle volume fraction, ambient temperature, and saturation on heat and mass transfer on the drying process. This study brings the effect of the presence of nanofluids in porous media. It contributes not only to our fundamental understanding of drying processes but also provides practical insights that can guide the development of more efficient and sustainable drying technologies.

Keywords

Mixed Convection, Heat Transfer, Nanofluid, Drying, Porous Media

1. Introduction

Fluid flow and heat transfer in porous media have been the subject of numerous investigations in the recent years [1] [2] [3] [4] due to its wide applications in engineering as heat exchangers, drying processes, geothermal and oil recovery, solar collectors, building construction, etc. In recent years, nanofluids have been an active field of research due to its greatly enhanced thermal properties. Nanofluid is a fluid containing nanometer sized particles (diameter less than 100 nm) or fibers suspended in traditional fluids such as water, ethylene glycol and oil. Choi was the first who proposed the term "nanofluid" [5]. The characteristic

feature of a nanofluid is the thermal conductivity enhancement reported by Masuda *et al.* [6]. The presence of small amount of nanoparticles (Al_2O_3-TiO_2) in the fluid increases the thermal conductivity of the fluid.

The use of nanofluids in a porous medium constitutes an emerging topic. Only a few researches have been performed in this area of free convection case. Nield and Kuznetsov [7] analyzed the free convection boundary layer flow in a porous medium saturated by a nanofluid. The model used for the nanofluid incorporates the effects of Brownian motion and thermophoresis. It was reported that the Brownian motion and thermophoresis parameters significantly influenced the reduced Nusselt number. Later, Kuznetsov and Nield [8] examined the natural convective heat transfer in the boundary layer flow of a nanofluid past a vertical flat plate embedded in a viscous fluid. Ahmad and Pop [9] investigated mixed convection boundary layer flow from a vertical flat plate embedded in a porous medium filled with nanofluids. They used the nanofluid model proposed by Tiwari and Das [10]. Hajipour and Dehkordi [11] studied mixed convection heat transfer of nanofluids in a vertical channel partially filled with porous medium. They used the Brinkman-Forchheimer model. The results found that increasing the nanoparticle concentration did not show a significant effect on the pressure drop. The nanofluid outlet temperature decreases with an increase in the Reynolds number value. Free convection about a vertical flat plate embedded in a saturated porous medium at high Rayleigh numbers was studied by Cheng and Minkowycz [12]. Arfin *et al.* [13] have examined the effect of three types of nanoparticles such as alumina (Al_2O_3), copper (Cu) and titania (TiO_2) on free and mixed convection boundary layer flow past a horizontal flat plate embedded in a porous medium saturated by a nanofluid. They used the nanofluid model proposed by Tiwari and Das, where this nanofluid model analyses the behaviour of nanofluids taking into account the solid volume fraction.

The effect of thermal radiation on mixed convection boundary layer flow over an isothermal vertical cone embedded in a porous medium saturated by a nanofluid was examined by Chamkha *et al.* [14]. Aziz *et al.* [15] found the numerical solution for steady boundary layer free convection flow past a horizontal flat plate embedded in a porous medium filled by a nanofluid containing gyrotactic microorganisms. The effect of bio-convection parameters was investigated. The results show that bio-convection parameters strongly influence the heat, mass and motile microorganism transport rates. Nazar *et al.* [16] studied mixed convection boundary layer flow over an isothermal horizontal cylinder embedded in a porous medium filled with a nanofluid. The effect of three different types of nanoparticles, namely Cu, Al_2O_3 and TiO_3, and their volume fraction on the flow and heat transfer was examined. Results showed that the increases of nanoparticle volume fraction decrease the magnitude of the skin friction coefficient. Cu gives the largest values of the skin friction coefficient followed by TiO_2 and Al_2O_3. Uddin and Harmand [17] have numerically investigated the natural convection heat transfer of nanofluids along the isothermal vertical plate embedded in a porous medium. Six different types of nanoparticles such as alumina Al_2O_3,

CuO, and TiO_2 with a valid range of particle concentration and particle size, have been taken with two base fluids. Results show that heat transfer rate increases with the increase in particle concentration. Keita *et al.* [18] have experimentally investigated drying colloidal particles suspended in a porous medium. They used MRI technique allowing to observe simultaneously the distributions of air, liquid, and colloid through the unsaturated solid porous structure. They have shown that the above phenomenon comes from a receding-front effect: The elements migrate towards the free surface of the sample and accumulate in the remaining liquid films. Pippal and Bera [19] studied natural convection in porous enclosure saturated with a copper-water nanofluid, whose two vertical walls are maintained at constant heat flux, while horizontal walls are adiabatic. They analyzed the effect of the Rayleigh number, Aspect ratio, solid volume fraction of nanoparticles and shape factor of nanoparticles. Results show that significant heat transfer enhancement can be obtained due to the presence of nanoparticles. Al-Hafidh and Mohammed [20] investigated the heat transfer by natural convection of nanofluid (Water-Cu) in a vertical cylindrical channel filled with porous media. The main objective was to study the influence of several pertinent parameters such as Rayleigh number, aspect ratio and the volume fraction on the heat transfer performance of nanofluids. The results indicate that with an increase of φ from 0.01 to 0.2, a rise of 50.4% for $Ra = 1000$ in the mean Nusselt number is observed. The ability to lose and gain heat at a fast rate of speed is greatly enhanced by adding nanomaterials to heat transfer compounds, which is one of the most significant new approaches for increasing heat transfer. Because of the significance of this industry and its influence on many other fields, heat transfer is the most significant area where nanomaterials have triggered an industrial revolution [21]-[26].

Research on the mixed convection heat and mass transfer within a porous medium containing nanofluid is notably limited. This scarcity underscores the significance of endeavors aimed at understanding such intricate phenomena. Based on previous research referenced as [27], the current study aims to address this deficiency by utilizing numerical techniques to examine the dynamics of heat and mass transfer throughout the mixed convective drying phase of a porous wall containing nanofluid. By exploring this complex interaction, the research aims to provide valuable insights into the behiavor of nanofluid within porous media during drying, thereby advancing the comprehension of this crucial process and its potential applications.

2. Basic Formulation

2.1. Case Study

The considered physical system in this work is sketched in **Figure 1**. It is a two-dimensional unsaturated porous vertical wall composed of an inert and rigid solid phase, a nanofluid phase (Water-Al_2O_3 or Water-Cu) and a gas phase which contains both air and water vapor. The left vertical face as well as the upper

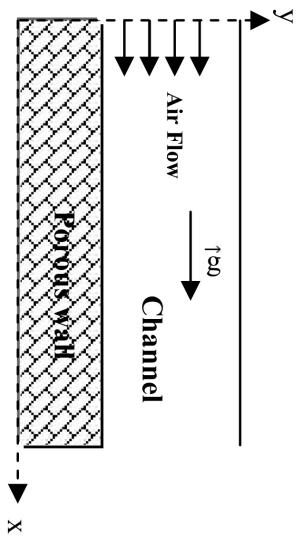

Figure 1. Physical problem.

and the bottom faces of the porous vertical wall face are assimilated to adiabatic and impervious faces. The right vertical face of the porous vertical wall is the permeable interface of the vertical channel. The porous vertical wall is submitted to an external downward lamina flow of water vapor mixture with controlled inlet variables wall. This porous wall is characterized by the following parameters: $\varepsilon = 0.26$, $\rho_s = 2600$ Kg·m^{-3}, $c_{ps} = 879$ J·Kg^{-1}·K^{-1}, $\lambda_s = 1.44$ W·m^{-1}·K^{-1} and $K = 2.510^{-4}$ m^2.

2.2. Hypotheses

For mathematical formulation of the problem, which describes the heat and mass transfer processes, the following assumptions are taken into consideration:

- The viscous dissipation, the compression work and the Soret and Dufour effects are neglected.
- The solid, liquid and gas phases are in local thermodynamic equilibrium.
- The radiative transfer mode is neglected.
- The dispersion and tortuosity terms are interpreted as diffusion terms.
- The boundary-layer approximations are valid.
- The porous medium is homogenous and isotropic.
- The nanofluid is considered as one liquid phase.
- The nanoparticle volume fraction is constant.

3. Governing Equations

3.1. In the Channel

Taking into account the above assumptions, the governing equations for a steady, laminar and incompressible flow along a vertical channel with boundary layer and Boussinesq approximations are written as:

1) Mass Conservation Equation

$$\frac{\partial\left(\rho_g U\right)}{\partial x}+\frac{\partial\left(\rho_g V\right)}{\partial y}=0 \tag{1}$$

2) Momentum Equation

$$\rho_g U\frac{\partial U}{\partial x}+\rho_g V\frac{\partial U}{\partial y}=-\frac{\partial P_g}{\partial x}+\frac{\partial}{\partial y}\left(\mu_g\frac{\partial U}{\partial y}\right)-\rho_g\left(\beta\left(T-T_0\right)+\beta^*\left(C_v-C_{V0}\right)\right) \tag{2}$$

3) Heat Equation

$$\rho_g C_{pg}\left(U\frac{\partial T}{\partial x}\right)+V\frac{\partial T}{\partial y}=\frac{\partial}{\partial y}\left(\lambda_g\frac{\partial T}{\partial y}\right)+\rho_g D_v\left(c_{pg}-c_{pa}\right)\frac{\partial T}{\partial y}\frac{\partial C_v}{\partial y} \tag{3}$$

where $c_{pg}=\left(1-C_v\right)c_{pa}+C_v c_{pv}$.

4) Species Equation

$$\rho_g U\frac{\partial C_v}{\partial x}+\rho_g V\frac{\partial C_v}{\partial y}=\frac{\partial}{\partial y}\left(\rho_g D_v\frac{\partial C_v}{\partial y}\right) \tag{4}$$

3.2. Inside the Porous Media

1) Mass Conservation Equation

Assuming that the average density of this phase is not constant and the nanofluid density is constant, the mass conservation equation for nanofluid, gas and Vapor phases are respectively given by:

$$\frac{\partial\varepsilon_{nf}}{\partial t}+\nabla\left\langle V_{nf}\right\rangle=-\frac{\dot{m}_v}{\rho_{nf}} \tag{5}$$

$$\frac{\partial\left\langle\rho_g\right\rangle}{\partial t}+\nabla\left[\left\langle\rho_g\right\rangle^g\left\langle V_g\right\rangle\right]=\dot{m}_v \tag{6}$$

$$\frac{\partial\left\langle\rho_v\right\rangle}{\partial t}+\nabla\left[\left\langle\rho_v\right\rangle^v\left\langle V_v\right\rangle\right]=\dot{m}_v \tag{7}$$

2) Velocity Equation

The average velocities of nanofluid phase and gas phases are obtained using Darcy's law:

$$\left\langle V_{nf}\right\rangle=-\frac{KK_{nf}}{\mu_{nf}}\left[\nabla\left(\left\langle P_g\right\rangle^g-P_c\right)+\left\langle\rho_{nf}\right\rangle^g\right] \tag{8}$$

$$\left\langle V_g\right\rangle=-\frac{KK_g}{\mu_g}\nabla\left\langle P_g\right\rangle^g \tag{9}$$

3) Energy Conservation Equation:

$$\begin{aligned}&\frac{\partial}{\partial t}\left[\left\langle\rho c_p\right\rangle\left\langle T\right\rangle\right]+div\left[\left(\left\langle\rho_l\right\rangle^l c_{pl}\left\langle V_l\right\rangle+\sum_{k=a,v}\left\langle\rho_g\right\rangle^g c_{pk}\left\langle V_k\right\rangle\right)\left\langle T\right\rangle\right]\\&=div\left[\lambda_{eff}\,grad\left\langle T\right\rangle\right]-\left[\Delta H_{vap}^O-\left(c_{pv}-c_{pl}\right)\right]\left\langle T\right\rangle\dot{m}_v\end{aligned} \tag{10}$$

3.3. For the Nanofluids

- The density of nanofluid, the thermal diffusivity, the thermal conductivity,

dynamic viscosity and the effective thermal conductivity are respectively given by the following equations [27] [28] [29] [30]:

$$\rho_{nf} = (1-\varphi)\rho_f + \varphi\rho_{np} \tag{11}$$

$$\alpha_{nf} = \frac{\lambda_{nf}}{(1-\varphi)(\rho C_p)_f + \varphi(\rho C_p)_{np}} \tag{12}$$

$$\lambda_{nf} = \lambda_f \frac{\lambda_{np} + (n-1)\lambda_f - (n-1)(\lambda_f - \lambda_{np})\varphi}{\lambda_{np} + (n-1)\lambda_f + (\lambda_f - \lambda_{np})\varphi} \tag{13}$$

$$\mu_{nf} = \frac{\mu_f}{(1-\varphi)^{2.5}} \tag{14}$$

$$\lambda_{eff} = \left[\lambda_g^n \varepsilon_g + \lambda_{nf}^n \varepsilon_{nf} + \lambda_s^n (1-\varepsilon)\right]^{\frac{1}{n}} \tag{15}$$

- The Thermo-physical properties of fluid and nanoparticles are given in **Table 1**:

Table 1. Thermo-physical properties of the fluid base and nanoparticles [31].

Physical Properties	Fluid Base	Nanoparticles	
	Water	Cu	Al_2O_3
ρ (kg·m^{-3})	997.1	8933	3970
C_p (J·kg^{-1}·K^{-1})	4179	385	765
k (W·m^{-1}·K^{-1})	0.613	400	40
$\alpha \times 10^{-7}$ (m^2·s^{-1})	1.47	1163.1	1738.6

3.4. Initial and Boundary Conditions

1) For the fluid in the channel

- The fluid state variables at the channel entrance are considered as constant.
- Assuming that the interface channel-porous medium is semi-permeable, the longitudinal and transverse velocities of the gas phase are written as:

$$U = 0;\ V = -\frac{D_v}{1-C_v}\left(\frac{\partial C_v}{\partial y}\right) \tag{16}$$

- For the right face of the channel, the longitudinal and transverse velocities are zero.

The local interfacial evaporating mass flux is evaluated by the following equation:

$$\dot{m}_v = \rho_g V \quad \text{for } 0 \le C_v < 1 \tag{17}$$

- The right vertical plate of the channel is kept isotherm.

2) For the porous medium

- The porous medium is assumed to be in local thermodynamic equilibrium. The temperature, the gas pressure and the liquid saturation are uniform.

- On the permeable face (the right face), heat and mass fluxes are written as follows:

$$\lambda_{eff}\frac{\partial\langle T\rangle}{\partial y}+\Delta H_{vap}\left[\left\langle\rho_{nf}\right\rangle^{nf}\left\langle V_{nf}\right\rangle\right]_y=h_{tx}\left[T_0-\langle T\rangle\right] \tag{18}$$

$$\left[\left\langle\rho_{nf}\right\rangle^{nf}\left\langle V_{nf}\right\rangle+\left\langle\rho_v\right\rangle^{g}\left\langle V_v\right\rangle\right]_y=h_{mx}\left[\left\langle\rho_v\right\rangle^{g}-\rho_{v0}\right] \tag{19}$$

- On the adiabatic and impervious sides (the other faces), the mass and heat fluxes are equal zero
- The equilibrium vapor pressure is a function of the temperature and the nanofluid saturation [32]:

$$P_v=P_{vs}\exp\left(-\frac{2\sigma M_v}{rR\rho_{nf}T}\right) \tag{20}$$

4. Numerical Resolution

The numerical resolution of equations governing dynamic, heat, and mass transfer within the fluid channel is resolved by the finite difference method. This method involves converting the system of equations into an algebraic equation system. The resolution proceeds in a step-by-step manner along the outflow direction. The channel mesh is regular and rectangular. At each iteration, the unknown variables (temperature, vapor water concentration, and velocity) in column k+1 are computed using the known variables from column *k*, following an explicit scheme. Inside the porous medium, the equations are numerically solved using a finite volume method, utilizing the concept of control domains outlined by Patankar [33]. Inspired by Whitaker's theory [34], a mathematical model governing heat and mass transfer is established for the unsaturated porous medium. The flow area is devised into a grid of point $P_{i,j}$ with Δx and Δy spacing in the x and y-directions. The values of the physical scalar Φ at the point $P_{i,j}$. The discretization of the conservation equation inside and outside the porous medium leads to a system of algebraic equations that can be written in the following form:

$$A_{i,j}\Phi_{i,j}=B_{i,j}\Phi_{i,j+1}+C_{i,j}\Phi_{i,j-1}+D_{i,j}$$

where $A_{i,j}$, $B_{i,j}$, $C_{i,j}$ and $D_{i,j}$ depend on the thermo-physical properties. By using the Gauss elimination method, the above system can be written as:

$$\Phi_{i,j}=P_{i,j}\Phi_{i,j+1}+Q_{i,j}$$

where

$$P_{i,j}=\frac{B_{i,j}}{A_{i,j}-C_{i,j}P_{i,j-1}}\quad\text{and}\quad Q_{i,j}=\frac{D_{i,j}+C_{i,j}Q_{i,j-1}}{A_{i,j}-C_{i,j}P_{i,j-1}}$$

For a detailed description of the method and the discretization of different equations inside and outside the porous medium, the reader can refer to D. Helel [35].

5. Numerical Results

5.1. Time Evolution of Different State Variables inside the Porous Medium

Figure 2 depicts the time evolution of temperature and saturation of the nanofluid for the center node of porous wall for different values of nanoparticle volume fraction $\varphi = 0$ (pure water), 0.05 and 0.15. It is shown that the temperature decrease by increasing of nanoparticles volume fraction. This behavior arises from reductions in the pressure gradient during the use of (Water-Al_2O_3) and from the impacts of density and viscosity, growing with using the Al_2O_3 in the water. Physically, an increase in density reduces the liquid velocity which in turn results in a lower shear stress. In contrast, an increase in viscosity increases the shear stress. The liquid velocity decreases with adding the Al_2O_3 within the based fluid. This is due to an increase in the liquid density in the presence of Al_2O_3. As a result of this increase in the nanofluid density, a slower flow is observed. The saturation of nanofluid for the right upper corner node of porous wall inside the porous wall decreases depending on the time and becomes weak from $t = 12$ h. The saturation of nanofluid declines as the nanoparticles volume fraction decreases.

Pure water has the shortest isenthalpic drying phase and it is the first one that enters the hygroscopic domain compared with nanoparticle dispersed in based fluid. It is remarked that the decrease in volume fraction of nanoparticles decreases isenthalpic phase. The same results are obtained by Keita *et al.* [18] in the case of steady drying colloidal particles suspended in a porous medium.

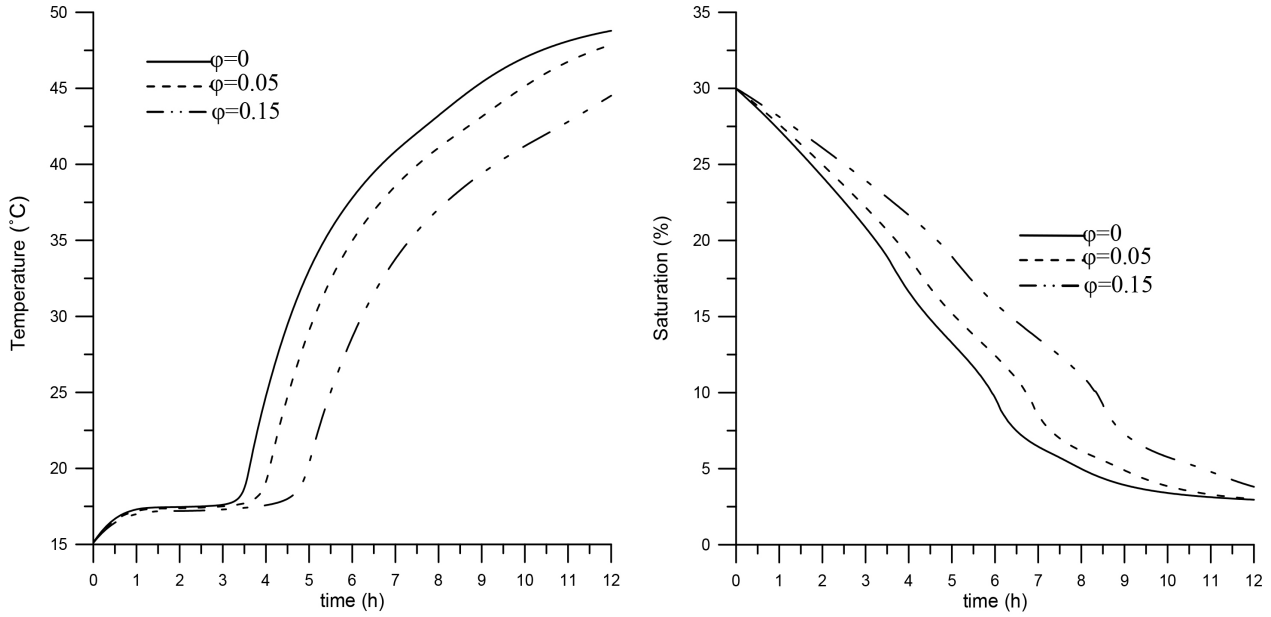

Figure 2. Time evolution of the temperature and the saturation of nanofluid for the centre node of porous wall for different volume fraction of Al_2O_3.

5.2. Evolution of the Effective Thermal Conductivity

Figure 3 is presented to show the effect of the volume fraction of nanoparticles on effective thermal conductivity. This figure illustrates the effect of different values of volume fraction, when the volume fraction of the nanoparticles increases from 0 to 0.15, the effective thermal conductivity rises. This contributes to reduce the temperature of the porous medium by approximately 4%. In Figure 4, the evolution of effective thermal conductivity with nanofluid (Water-Al_2O_3) saturation when the volume fraction of nanoparticle is equal to 0.15, is illustrated. It is evident from the graph that the effective thermal conductivity value rises as the saturation of nanofluid increases. This suggests that increased saturation levels result in improved conductivity within the nanofluid.

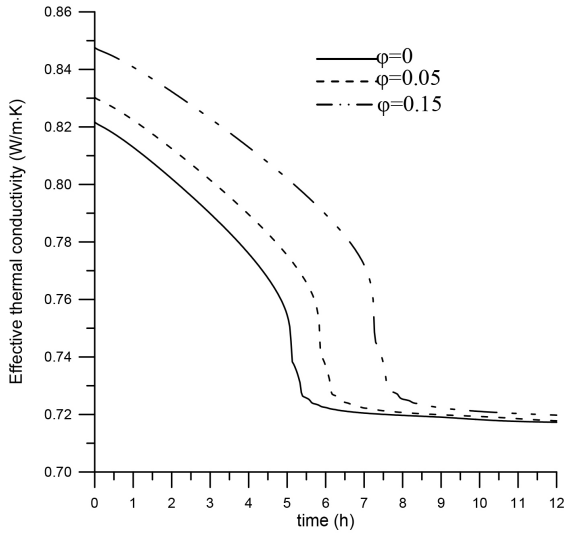

Figure 3. Time evolution of the effective thermal conductivity. Effect of Alumina volume fraction.

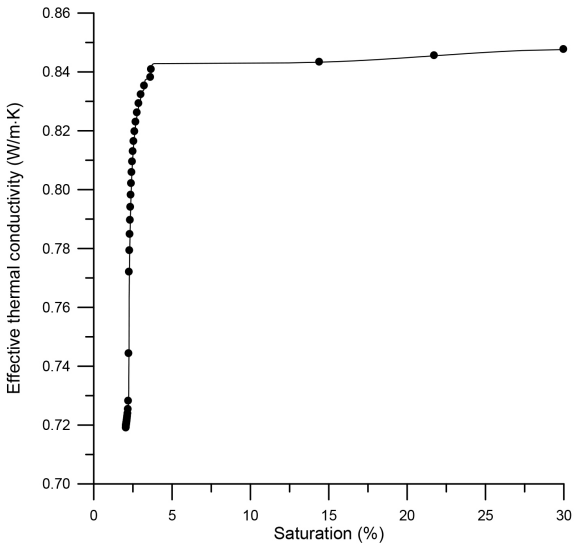

Figure 4. Evolution of effective thermal conductivity with nanofluid saturation.

5.3. Time Evolution of the Average Heat and Mass Transfer Coefficient

The results show that the average heat and mass transfer coefficient in the nanofluid (Water-Al_2O_3) is less than that in pure water. Figure 5 illustrates the effect of volume fraction of nanoparticles on the time evolution of the average heat and mass transfer coefficient for nanofluid. It is shown that the average heat and mass transfer coefficient was decreased by increasing volume fraction of nanoparticle.

5.4. Effect of the Ambient Temperature

Figure 6 shows the time evolution of temperature of nanofluid in the porous medium for several values of the ambient temperature for nanofluid (Water-Al_2O_3) when $\varphi = 0.05$. In the case where the temperature is 100˚C, the phenomenon of evaporation starts from the beginning and as a result, drying will be faster. The increase in ambient temperature decreases drying time and can even significantly reduce the duration of the second phase. The temperature of nanofluid increases with time gradually until it reaches the maximum value.

5.5. Effect of the Initial Saturation

Figure 7 depicts respectively, the time evolution of temperature and saturation of nanofluid for the alumina particles when $\varphi = 0.05$. It is clear that the second phase becomes shorter and can even disappear completely when the saturation of nanofluid decreases. This can be explained by the fact that from the beginning of the drying, the medium enters the field hygroscopic. For $S_{ini} = 20\%$, the temperature of the porous medium increases from the beginning, whereas $S_{ini} = 40\%$, it follows the conventional profile which is observed during the different phases.

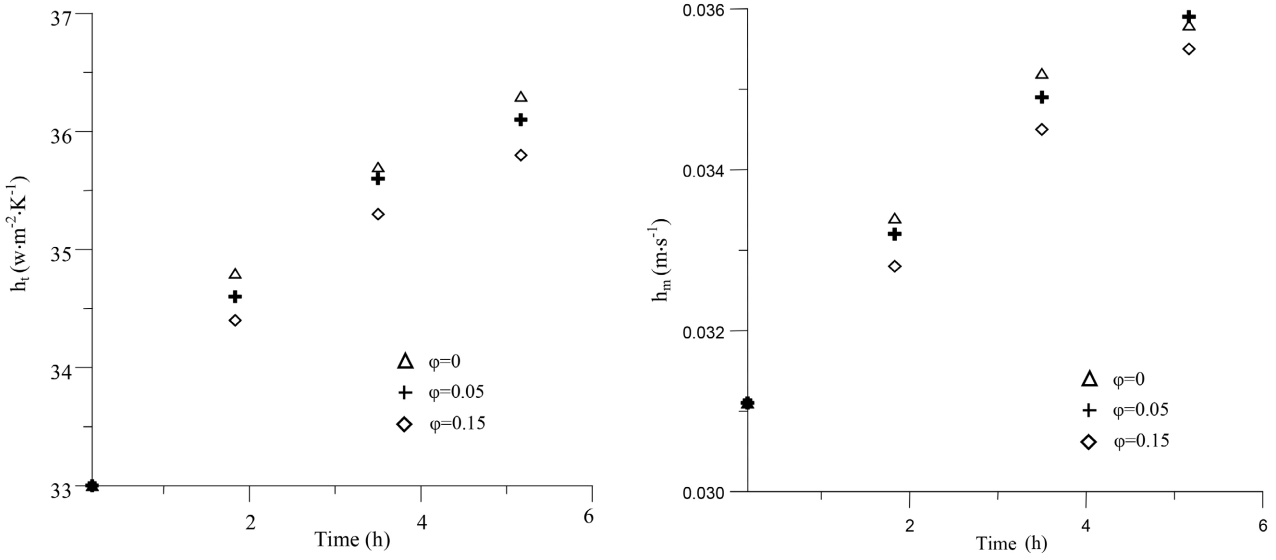

Figure 5. Time evolution of the average heat (h_t) and mass (h_m) transfer coefficient.

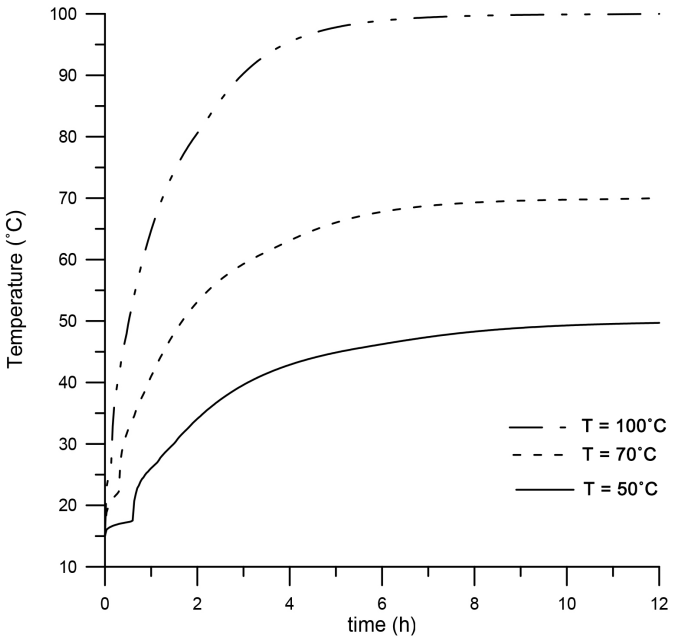

Figure 6. Time evolution of the temperature of nanofluid for the right upper corner node of porous wall. Effect to initial temperature.

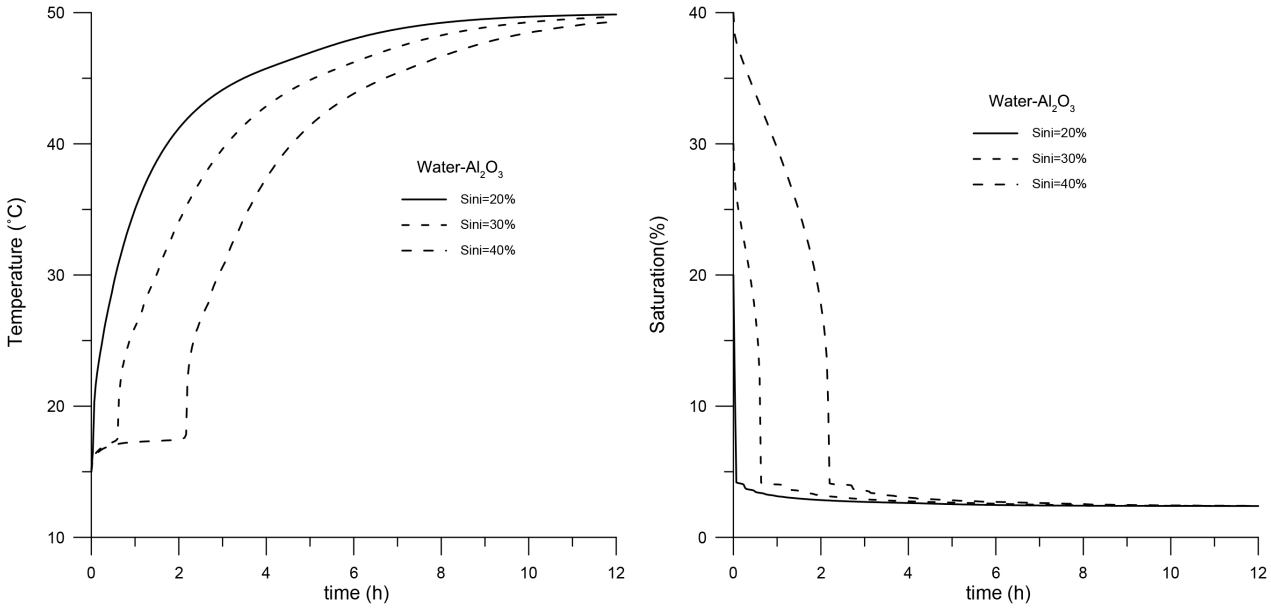

Figure 7. Time evolution of the temperature and the saturation of nanofluid for the right upper corner node of porous wall.

5.6. Effect of the Type of Nanoparticle

Figure 8 shows the evolution of temperature and saturation of nanofluid when φ = 0.05 for the right upper corner node of porous wall with time for two different types of nanoparticle. It is seen that the nanofluid Water-Al_2O_3 has a shorter drying time compared to the nanofluid Water-Cu. Drying velocity is higher in the case of (Water-Al_2O_3) than that in (Water-Cu) because density of (Water-Al_2O_3) is lower than density of (Water-Cu).

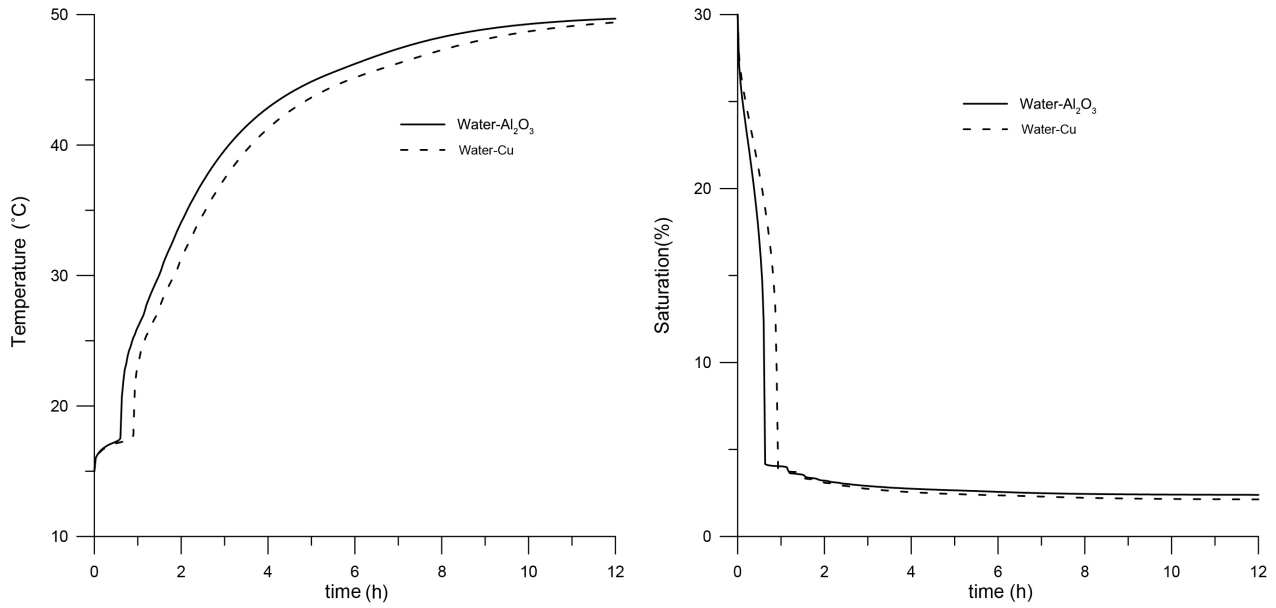

Figure 8. Time evolution of the temperature and the saturation of nanofluid for the right upper corner node of porous wall. Effect of the type of nanoparticles.

6. Conclusions

The present work concerns a numerical study of two-dimensional heat and mass transfer during mixed convective drying of unsaturated porous walls containing nanofluid. We have examined the effect of the nanoparticle volume fraction, the ambient temperature, the initial nanofluid saturation, the initial pressure and the type of nanoparticle on the heat and mass transfer. The main conclusions of this study are as follows:

- The effect of adding nanoparticles is very significant. The temperature of porous media decreases when the volume fraction of nanoparticles increases.
- The drying rate is substantially faster when using pure water compared to nanofluids.
- A comparative study demonstrates that suspended nanoparticles significantly increase the heat and mass transfer as the nanoparticles volume fraction. Both Cu and Al_2O_3 demonstrate this enhancement.

In the future, this study will investigate other types of base fluids and nanoparticles.

Conflicts of Interest

The authors declare no conflicts of interest regarding the publication of this paper.

References

[1] Nield, D.A. and Bejan, A. (2006) Convection in Porous Media. Springer.

[2] Ingham, D.B. and Pop, I. (2005) Transport Phenomena in Porous Media III. Elsevier.

[3] Vafai, K. (2005) Handbook of Porous Media. Taylor & Francis.

[4] Vadasz, P. (2008) Emerging Topics in Heat and Mass Transfer in Porous Media. Springer.

[5] Choi, S. (1995) Enhancing Thermal Conductivity of Fluids with Nanoparticles. In: Siginer, D.A. and Wang, H.P., Eds., *Developments and Applications of Non-Newtonian Flows*, FED-Vol. 231/MD-Vol. 66, ASME, 99-105.

[6] Masuda, H., Ebata, A., Teramae, K. and Hishinuma, N. (1993) Alteration of Thermal Conductivity and Viscosity of Liquid by Dispersing Ultra-Fine Particles. *Netsu Bussei*, **7**, 227-233. https://doi.org/10.2963/jjtp.7.227

[7] Nield, D.A. and Kuznetsov, A.V. (2009) The Cheng-Minkowycz Problem for Natural Convective Boundary-Layer Flow in a Porous Medium Saturated by a Nanofluid. *International Journal of Heat and Mass Transfer*, **52**, 5792-5795. https://doi.org/10.1016/j.ijheatmasstransfer.2009.07.024

[8] Kuznetsov, A.V. and Nield, D.A. (2010) Natural Convective Boundary Layer flow of a Nanofluid past a Vertical Plate. *International Journal of Thermal Sciences*, **49**, 243-247. https://doi.org/10.1016/j.ijthermalsci.2009.07.015

[9] Ahmad, S. and Pop, I. (2010) Mixed Convection Boundary Layer Flow from a Vertical Flat Plate Embedded in a Porous Medium Filled with Nanofluids. *International Communications in Heat and Mass Transfer*, **37**, 987-991. https://doi.org/10.1016/j.icheatmasstransfer.2010.06.004

[10] Tiwari, R.K. and Das, M.K. (2007) Heat Transfer Augmentation in a Two-Sided Lid-Driven Differentially Heated Square Cavity Utilizing Nanofluids. *International Journal of Heat and Mass Transfer*, **50**, 2002-2018. https://doi.org/10.1016/j.ijheatmasstransfer.2006.09.034

[11] Hajipour, M. and Dehkordi, A.M. (2014) Mixed-Convection Flow of Al_2O_3-H_2O Nanofluid in a Channel Partially Filled with Porous Metal Foam: Experimental and Numerical Study. *Experimental Thermal and Fluid Science*, **53**, 49-56. https://doi.org/10.1016/j.expthermflusci.2013.11.002

[12] Cheng, P. and Minkowycz, W.J. (1977) Free Convection about a Vertical Flat Plate Embedded in a Porous Medium with Application to Heat Transfer from a Dike. *Journal of Geophysical Research*, **82**, 2040-2044. https://doi.org/10.1029/JB082i014p02040

[13] Arifin, N., Nazar, R. and Pop, I. (2012) Free and Mixed Convection Boundary Layer Flow past a Horizontal Surface Embedded in a Porous Medium Filled with a Nanofluid. *AIAA Journal of Thermophysics and Heat Transfer*, **26**, 375-382. https://doi.org/10.2514/1.T3645

[14] Chamkha, A.J., Abbasbandy, S., Rashad, A.M. and Vajravelu, K. (2013) Radiation Effects on Mixed Convection over a Wedge Embedded in a Porous Medium Filled with a Nanofluid. *Transport in Porous Media*, **91**, 2061-1279.

[15] Aziz, A., Khan, W.A. and Pop, I. (2012) Free Convection Boundary Layer Flow past a Horizontal Flat Plate Embedded in Porous Medium Filled by Nanofluid Containing Gyrotactic Microorganisms. *International Journal of Thermal Sciences*, **56**, 48-57. https://doi.org/10.1016/j.ijthermalsci.2012.01.011

[16] Nazar, R., Tham, L., Pop, I. and Ingham, D.B. (2011) Mixed Convection Boundary Layer Flow from a Horizontal Circular Cylinder Embedded in a Porous Medium Filled with a Nanofluid. *Transport in Porous Media*, **86**, 517-536. https://doi.org/10.1007/s11242-010-9637-1

[17] Ziya, U. and Souad, H. (2013) Natural Convection Heat Transfer of Nanofluids along a Vertical Plate Embedded in Porous Medium. *Nanoscale Research Letters*, **8**,

Article No. 64.

[18] Keita, U., Faure, P., Rodts, S. and Coussot, P. (2013) MRI Evidence for a Receding-Front Effect in Drying Porous Media, *Physical Review*, **87**, Article ID: 062303.

[19] Zhang, L.Y., *et al.* (2021) Numerical Study of Natural Convection Heat Transfer in a Porous Annulus Filled with a Cu-Nanofluid. *Nanomaterials*, **11**, Article No. 990. https://doi.org/10.3390/nano11040990

[20] Manal, H.A.H. and Hayder, I.M. (2013) Natural Convection of Nanofluid in Cylindrical Enclosure Filled with Porous Media, *Journal of Power and Energy Engineering*, **7**, 2263-2272.

[21] Jadhav, M.M.P., Jadhav, D.B. and Nimgade, M.E. (2017) Heat Transfer Enhancement Using Nanofluids in Automotive Cooling System. 3*rd International Conference on Ideas*, *Impact and Innovation in Mechanical Engineering* (*ICIIIME* 2017), Volume 5, 1035-1042.

[22] Buongiorno, J. and Hu, L. (2009). Nanofluid Heat Transfer Enhancement for Nuclear Reactor Applications. *ASME* 2009 *Second International Conference on Micro/Nanoscale Heat and Mass Transfer*, Volume 3, 517-522. https://doi.org/10.1115/mnhmt2009-18062

[23] Huminic, G. and Huminic, A. (2012) Application of Nanofluids in Heat Exchangers: A Review. *Renewable and Sustainable Energy Reviews*, **16**, 5625-5638. https://doi.org/10.1016/j.rser.2012.05.023

[24] Li, Y., Shakeriaski, F., Barzinjy, A.A., Dara, R.N., Shafee, A. and Tlili, I. (2019) Nanomaterial Thermal Treatment along a Permeable Cylinder. *Journal of Thermal Analysis and Calorimetry*, **139**, 3309-3315. https://doi.org/10.1007/s10973-019-08706-7

[25] Lotfizadeh, S. and Matsoukas, T. (2015) Effect of Nanostructure on Thermal Conductivity of Nanofluids. *Journal of Nanomaterials*, **2015**, Article No. 8.

[26] Moradi, A., Toghraie, D., Isfahani, A.H.M. and Hosseinian, A. (2019) An Experimental Study on MWCNT-Water Nanofluids Flow and Heat Transfer in Double-Pipe Heat Exchanger Using Porous Media. *Journal of Thermal Analysis and Calorimetry*, **137**, 1797-1807. https://doi.org/10.1007/s10973-019-08076-0

[27] Dalel, H., Lefi, N. and Boukadida, N. (2009) Mixed Convection in a Vertical Channel Flow during Drying Process. *International Journal of Heat and Technology*, **27**, 67-76.

[28] Khanafer, K., Vafai, K. and Lightstone, M. (2003) Buoyancy-Driven Heat Transfer Enhancement in a Two-Dimensional Enclosure Utilizing Nanofluids. *International Journal of Heat and Mass Transfer*, **46**, 3639-3653. https://doi.org/10.1016/s0017-9310(03)00156-x

[29] Xuan, Y. and Li, Q. (2003) Investigation on Convective Heat Transfer and Flow Features of Nanofluids. *Journal of Heat Transfer*, **125**, 151-155. https://doi.org/10.1115/1.1532008

[30] Brinkman, H.C. (1952) The Viscosity of Concentrated Suspensions and Solutions. *The Journal of Chemical Physics*, **20**, 571-581. https://doi.org/10.1063/1.1700493

[31] Mobarki, A., Boukadida, N. and Ben Nasrallah, S. (2003) The Variability Effect of Fluid Thermophysical Properties on Convective Drying of Unsaturated Porous Media. *International Journal of Heat and Technology*, **21**, 89-97.

[32] Oztop, H.F. and Abu-Nada, E. (2008) Numerical Study of Natural Convection in Partially Heated Rectangular Enclosures Filled with Nanofluids. *International Journal of Heat and Mass Transfer*, **29**, 1326-1336.

[33] Patankar, S.V. (1980) Numerical Heat and Fluid Flow. Hemisphere.

[34] Whitaker, S. (1977) Simultaneous Heat Mass and Momentum Transfer in Porous Media: A Theory of Drying. In: *Advances in Heat Transfer*, Academic Press, Vol. 13, 119-203. https://doi.org/10.1016/S0065-2717(08)70223-5

[35] Dalel, H., Lefi, N. and Noureddine, B. (2013) Effect of Metrological Temperature on Vertical Porous Wall Drying Process in Forced and Mixed Convection. *International Journal of Heat and Technology*, **31**, 75-83.

Nomenclature

C_v: Water vapor concentration
C_p: Specific heat at constant pressure ($J \cdot kg^{-1} \cdot K^{-1}$)
C_{ps}: Specific heat of porous medium, ($J \cdot kg^{-1} \cdot K^{-1}$)
D_v: Vapor diffusion coefficient into air ($m^2 \cdot s^{-1}$)
E: Channel width (m)
G: Gravitational constant, $m \cdot s^{-2}$
Gr_m: Mass transfer Grashof number
Gr_t: Heat transfer Grashof number
H: Channel height (m)
h: Hour
h_m: Average mass transfer coefficient ($m \cdot s^{-1}$)
h_t: Average heat transfer coefficient ($W \cdot m^{-2} \cdot K^{-1}$)
K: Permeability of porous medium (m^2)
l: Thickness of porous wall (m)
M: Molecular weight (Kg)
$\dot{m}_v$: Mass rate of evaporation ($Kg \cdot m^{-2} \cdot s^{-1}$)
P: Pressure (Pa)
P_c: Capillary pressure, Pa
R: Universal gas constant ($J \cdot mole^{-1} \cdot K^{-1}$)
r: Curve ray, m
S: Saturation (%)
T: Temperature, K
t: Time (s)
U, V: Velocity components in x, y directions ($m \cdot s^{-1}$)

Greek Symbols

α: Thermal diffusivity of the nanofluid ($m^2 \cdot s^{-1}$)
β: Coefficient of thermal expansion (K^{-1})
β': Coefficient of mass expansion
ε: Volume fraction
λ: Thermal conductivity ($W \cdot m^{-1} \cdot K^{-1}$)
μ: Dynamic viscosity ($Kg \cdot m^{-1} \cdot s^{-1}$)
ρ: Density ($Kg \cdot m^{-3}$)
σ: Superficial tension, $N \cdot m^{-1}$
φ: Nanoparticle volume fraction

Subscripts

a: Dry air
eff: Effective
g: Gas (air-water vapor mixture)
ini: Initial
int: Interface
l: Liquid
o: Ambient
s: Solid
v: Water vapor
vs: Saturated vapor
x: Local
f: fluid base
nf: Nanofluid
np: Nanoparticle